NASA TECHNICAL MEMORANDUM
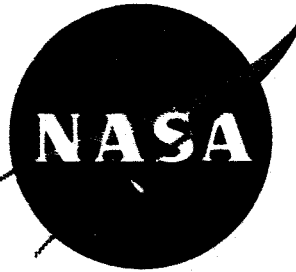
NASA NASA TM X-52152

NASA TM X-52152

GPO PRICE $ _____

CFSTI PRICE(S) $ _____

Hard copy (HC) _1.00_

Microfiche (MF) _.50_

ff 653 July 65

SAHA-LANGMUIR SURFACE IONIZATION RELATION

by Roland Breitwieser and Wayne Rush

Lewis Research Center

Cleveland, Ohio

NATIONAL AERONAUTICS AND SPACE ADMINISTRATION · WASHINGTON, D.C. · 1965

SAHA-LANGMUIR SURFACE IONIZATION RELATION

by Roland Breitwieser and Wayne Rush

Lewis Research Center
Cleveland, Ohio

SAHA-LANGMUIR SURFACE IONIZATION RELATION

Roland Breitwieser and Wayne Rush

Lewis Research Center
National Aeronautics and Space Administration
Cleveland, Ohio

Abstract

27489

The experimentally observed ion production rate in a cesium thermionic converter with tungsten electrodes is 3 to 4 times the rate predicted by the Saha-Langmuir equation. The ion emission rate is found to be dependent on field and corresponds to an $\exp\left(e\sqrt{eE}/kT\right)$ (Schottky) relation. The Schottky effect is unambiguous only at very small spacings (3 to 11μ) and at conditions of low ionization probabilities. Agreement between ion current and simple space-charge theory is observed. This agreement and the departure from the Saha-Langmuir relation suggest that the ions are formed at localities of higher work function than the electrons. The difference in work function for ion and electron production thus reduces the effectiveness of ions in reducing the space charge of electrons at the electron-saturation condition. Observations on the coupling of ion motion to particle arrival rate are also made.

Introduction

Author

The "ideal" passive-mode thermionic converter (one in which volume ionization does not occur) is still an important objective in thermionic conversion. It is probable that surface ionization will play a significant role in thermionic conversion if an effective passive-mode operation is to be achieved. This paper presents observations on ion production probability, the Schottky effect on ion generation, space-charge effects, and the coupling of ion motion with arrival rates.

Symbols

A	24, constant in eq. (A6)	ϵ	0.577, constant in eq. (A6)
B	1.5, constant in eq. (A6)	θ	angle
E	field	κ	2.492, constant in eq. (A6)
e	electronic charge	μ	free energy
$\mathcal{F}$	function	μ_a	free energy of atoms
h	Planck's constant	μ_e	free energy of electrons
J	current	μ_p	plasma potential
J_o	zero field satuation current	μ_+	free energy of ions
k,k'	Boltzmann constant	ν	particle flux
m	mass	ν_a	atom flux
n	number density	ν_e	electron flux
n_a	number density of neutral atoms	ν_{ep}	electron flux from plasma
n_e	number density of electrons	ν_{es}	electron flux from surface
n_+	number density of positive ions	ν_+	ion flux
p	pressure	ρ	dimensionless density
Q	partition function	σ	cross section
Q_a	partition function for atoms	σ_m	total cross section
Q_e	partition function for electrons	$\sigma_{+,m}$	energy-dpendent momentum, transfer cross section
Q_+	partition function for positive ions		
q	electronic charge	φ	work function
r_a	atom reflection coefficient	φ_1	emitter work function
r_+	ion reflection coefficient	φ_2	collector work function
T	temperature	X	dimensionless distance
T_{cs}	cesium reservoir temperature	ψ	dimensionless potential
T_1	emitter temperature		
V	voltage		
V_i	ionization potential		
x	distance		
α	ratio of ion particle flux to atom particle flux		

Analytical Relations

The relations given in Appendix A relate to ion emission and ion transport and are commonly used in thermionics. To facilitate the review of the experimental results, however, a brief resume of the Saha-Langmuir equation is presented.

The Saha-Langmuir equation is based on the equilibrium between an ionized gas (plasma) and the containing surface. The flux of the electron gas from the metal containing surface must be equal to the electron flux from the plasma. For the sake of simplicity, it is assumed that the body of the plasma and the plasma near the surface are at the same potential as the surface ($\mu_p = e\varphi$). The Saha equilibrium equation is then used to define the relative particle concentrations in the plasma. The expression for the free energy of this system is

$$\mu_a = \mu_+ + \mu_e + eV_i \tag{1}$$

Substituting equation (A9) in equation (1) results in

$$\frac{n_+ n_e}{n_a} = \frac{Q_+ Q_e}{Q_a} \left(\frac{2\pi\, m_e kT}{h^2} \right)^{3/2} \exp\left(-\frac{eV_i}{kT} \right) \tag{2}$$

In terms of particle flux, since $\nu = n\sqrt{\dfrac{kT}{2\pi m}}$, $\tag{3}$

$$\frac{\nu_+ \nu_{e,p}}{\nu_a} = \left(\frac{kT}{2\pi m_e} \right)^{1/2} \left(\frac{2\pi\, m_e kT}{h^2} \right)^{3/2} \exp\left(-\frac{eV_i}{kT} \right) \tag{4}$$

The equivalent development of the Richardson-Dushman equation for the electron gas in the metal with its surroundings[1] results in

$$\nu_{es} = \frac{4\pi\, m_e (kT)^2}{h^3} \exp\left(-\frac{e\varphi}{kT} \right) \tag{5}$$

Equating the surface and plasma electron fluxes ($\nu_{es} = \nu_{ep}$) and solving for the ratio of ion to atom flux yield the Saha-Langmuir equation

$$\frac{\nu_+}{\nu_a} = \frac{\sqrt{kT/2\pi m}_e (2\pi m_e kT/h^2)^{3/2} \exp\left(-eV_i/kT \right)}{4\pi m_e [(kT)^2/h^3] \exp - (e\varphi/kT)} \tag{6}$$

$$= 1/2 \ \exp\left[\frac{e(\varphi - V_i)}{kT} \right] \tag{7}$$

At equilibrium, the flow to the surface and away from the surface for each particle is, of course, equal. Many refinements to the Saha-Langmuir equation exist. For example, consideration of particle reflection (treated by Copely and Phipps[2]) results in

$$\frac{\nu_+}{\nu_a} = \frac{(1 - r_+)}{(1 - r_a)} \ \frac{1}{2} \ \exp\left[\frac{e(\varphi - V_i)}{kT} \right] \tag{8}$$

The effect of field on surface ionization has also been treated in a survey article by Zanberg and Ionov,[3] in which Morgulis (1934) is credited with first observing the field effect on surface ionization, and Dobretsov (1936) is credited with relating the ion production enhancement to the change in image field (analogous to the Schottky effect).

The simple equilibrium approach used in equation (6) can be continued to include these field effects by first assuming that the plasma potential is not equal to the surface potential. The number density of the particles in the plasma is still described by equation (2).

Matching the plasma fluxes to surface fluxes at equilibrium requires that the Boltzmann relation (eq. (A3)) be maintained. Thus the potential corresponding to the increased charge density, $\mu_p < e\varphi$, or reduced charge density, $\mu_p > e\varphi$, must match at the surface where μp equals $e\varphi_{eff}$. Since equilibrium constraints are still employed, the relative flux rates are yet described by equation 4. It follows that a plasma sheath must exist to permit matching the plasma boundary conditions with the surface boundary conditions. (These relations have been observed and evaluated numerically by Nottingham[4] in his isothermal diode paper.)

Since equation (4) applies, equation (6) must apply. But the application of equation (6) to the case where μ_p is less than $e\varphi$ produces a strong electron accelerating field away from the surface. The work function φ is modified for the effect of the field (the Schottky effect - Nottingham[4]). Equation (6) then becomes

$$\frac{\nu_+}{\nu_a} = \frac{\left(\frac{kT}{2\pi m_e}\right)^{1/2}\left(\frac{2\pi\, m_e kT}{h^2}\right)^{3/2}\exp - (eV_i/kT)}{4\pi m_e [(kT)^2/h^3](\exp - \varphi e/kT)[\exp (e\sqrt{eE}/kT)]} \qquad (9)$$

Cancelling terms as before results in

$$\frac{\nu_+}{\nu_a} = \frac{1}{2}\exp\left[(e\varphi - eV_i - e\sqrt{eE})/kT\right] \qquad (10)$$

for fields that accelerate surface electrons. By analogy, a similar image force relation should occur for a field that accelerates the positively-charged ions. The effective work function barrier that determines charge flux would then be increased by an amount

$$\Delta\varphi = e\sqrt{eE}/kT \qquad (11)$$

and equation (10) would become

$$\frac{\nu_+}{\nu_a} = \frac{1}{2}\exp\left[(e\varphi - eV_i + e\sqrt{eE})/kT\right] \qquad (12)$$

for a field that accelerates ions.

The Saha-Langmuir equation can be extended to include "patchy" (variable work function) surfaces. The various formalisms, while not complex, are bulky, so they will not be repeated here (see Zandberg and Ionov[3] or Kaminsky[5]). Zandberg has indicated that field as high as 10^6 V/m may be necessary to eliminate "interpatch" effects in field-enhanced surface-ionization studies.

The equilibrium-based equations appear to be reasonably supported by experiment (Kaminsky[5] and Zandberg and Ionov[3]). Although considerable contradictions exist in past literature on the field effect on surface ionization, a more recent study by Zandberg and Ionov[6] support the $e\sqrt{eE}/kT$ dependence. Less well established are surface-ionization studies at conditions encountered in thermionic conversion, that is, high-fractional cesium coverage and low ionization probability.

Apparatus and Procedure

The various features of the planar variable-spacing diode are essentially as described in detail by Breitwieser[7]. The 1.5-centimeter-diameter emitter was formed from tungsten oriented to expose the 110 (Miller index) plane. Several crystals composed the face, but the maximum misorientation was only $1\frac{1}{2}°$. A post-mortem examination disclosed some surface reorientation to the crystal faces. The body of emitter subsurface retained a 110 orientation. It is not clear whether the surface reorientation existed during the tests or was a result of damage incurred as the tests were terminated by a leak.

A refinement to the operating procedure previously described[7] was the method of use of the collector guard and an associated high-gain differentially coupled amplifier. Improved current resolution in the microampere range resulted.

Presentation of Data

Figure 1 illustrates the comparison of experimental ion currents with ion currents calculated by equation (12). The evaluation of work function was determined through the Richardson Dushman equation (A1). The experimental data were extrapolated back to the zero-field condition through the use of the Schottky relation (A2). The observed data were obtained at conditions corresponding to field strengths up to 3.5×10^6 V/m. The data shown were obtained at spacings estimated to be 3-11 μ. Knudsen flow was assumed in calculating the arrival rates in the analytical estimates.

Figure 2 is a typical Schottky plot taken at an emitter temperature of 1530° K, at a cesium reservoir temperature of 470° K, and at three interelectrode spacings. The condition of operation would correspond to an ion-rich condition at the emitter on the basis of the Saha-Langmuir equation (A4) in which the emitter work function is determined from the saturated current of electrons. The quantity $V - 1$ in the abscissa adjusts the applied voltage V to the surface potential difference ($\varphi_1 - \varphi_2 \approx 1$). The smallest spacing is estimated to be 3 to 11 μ on the basis of external measurement. The Schottky slope indicates a spacing of 10 μ. The vertical lines labeled zero-field potentials were calculated by using the Langmuir space-charge relation for singly charged cesium ions (eq. (A8)). No electron neutralization was assumed. The extrapolated zero-field ion current based on the Schottky analysis for the closest spacing data was used in the dimensionless distance relation for all spacings (eq. (A8)). The resulting values of voltage to produce the zero field are plotted as vertical lines. The dashed vertical line indicates the region where the electron current would be expected to have a significant effect on the net current, as estimated from close-spacing data.

Figure 3 is similar to figure 2. The temperatures shown correspond to a slightly electron-rich condition at the emitter on the basis of the Saha-Langmuir theory and electron currents but slightly ion-rich on the basis of the observed currents. Again, the small-spacing Schottky slope (10 μ) corresponds to the measured values for the closest spacing (3 to 11 μ). The potentials required to produce a zero field at the emitter (single-charge theory) intercept the actual data to indicate a consistency in zero field currents.

Figure 4 is similar to the two previous figures. The emitter temperature is 1600° K, and the cesium temperature is 530° K. Thus, the probability of ion-neutral collision is greater. Included in figure 4 are runs that represent the level of data scatter involved in successive (days or weeks) runs. The results are similar to results presented in figures 2 and 3 except that the zero field potentials do not intercept at the same value of ion-current density.

Figure 5 is a plot of the logarithm of current as a function of applied voltage. The interelectrode spacing was 3 to 11 μ. The emitter temperature of 2007° K and the cesium reservoir temperature of 309° K were selected to ensure nearly complete ionization of the arriving particles ($\exp [e(\varphi - V_i)/kT] >> 1$). It was anticipated that these conditions would yield information on particle arrival rates and thus clarify some aspects of the deviations of ion current from the Saha-Langmuir theory. The results indicated instead that a coupling exists between ion motion and arrival rate.

Two theoretical curves were superimposed on the experimental data. The higher values of theoretical ion current were based on free-molecule (Knudsen) flow. It was assumed the flux rate above the cesium reservoir, as calculated by the vapor pressure relation of Heimel[8] (eq. (A7)), was identical to the flux in the interelectrode space (Knudsen flow). The theoretical curve was corrected for ion space charge by the method of Nottingham and Breitwieser[9] The lower theoretical values of ion current assume that the interelectrode space is at the same pressure as the surrounding gas. It was further assumed that the momentum exchange was primarily between the surrounding gas (assumed at T_{cs}) and the ions in the interelectrode space. Thus the flux in the interelectrode space was reduced by the ratio of $\sqrt{T_{cs}/T_1}$.

Qualitative agreement between the ion-current and constant-pressure arrival rates exist at the low retarding voltages customarily used in thermionic converter studies (-3 to -8 V), but at high retarding voltages (-30 to -40 V) the Knudsen flow provides a more adequate comparison.

Figures 6 and 7 are extensions of figure 5, in which the same comparisons are made at larger spacings. In some cases the complete development of the theoretical curve was terminated at the condition of zero field at the emitter, thus avoiding the tedious space-charge calculations. It should be noted the cesium reservoir temperature varied from 325° to 329° K in these tests; thus the slight difference in the value of the saturated ion current. All sets of data in figures 5, 6 and 7 show the same general trend. The observed ion currents at -30 to -40 volts correspond to the Knudsen predictions. Currents measured at 1 to 2 volts more negative than the theoretical zero-field condition at the emitter correspond to the constant-pressure predictions.

Discussion of Results

Although the magnitude of the experimentally observed ion current is greater than that predicted by the Saha-Langmuir equation, the close agreement to the functional form of the equation is indeed surprising in view of the equation's equilibrium origin. The departure from equilibrium, while not great for electron emission, would appear to be a major perturbation in the case of ion emission, particularly at high fields. The experimental values are consistently only 3 to 4 times that predicted by the Saha-Langmuir relation. Possible reasons for the departure are many. Experimental errors in temperature measurements, such as emitter and cesium reservoir, were explored but could not adequately explain the deviation. Arrival-rate discrepancies, based on the various cesium vapor pressure relations or distortion in local fluxes, were insufficient or in the wrong direction to explain the higher ion-production probability, as indicated in the particle arrival-rate studies illustrated in figures 5, 6 and 7.

One self-consistent possibility exists: the work function effective in producing ions may be higher than that related to the emission of electrons. For, example, a difference of 1.2 e/kT (the eV equivalence of emitter temperature) would account for the difference between experiment and theory shown in figure 1 if equal areas for ion and electron emission are assumed. This difference in surface potential level then could reduce the electron current (and thus electron density) at the zero-field condition for ion emission sufficiently to permit the use of the single-species space-charge theory. The justification for the use of this space-charge analysis was in part established by examining the analytical mixed-charge space-charge results of Goldstein[10,11]. The results indicate that if the ion emission density is about 10 times the electron emission density, the single-species space-charge theory is adequate to determine the zero-field emission condition. At low values of X (eq. (A8)) the approximation improves.

Since the results in figures 2 and 4 correspond to an ion-rich emission density condition (based on the application of the Saha-Langmuir relation to the work function calculated from electron current), an additional barrier of 1.2 e/kT should then allow the experimental results to approach the required ion to the electron emission density ratio of 10. However, the conditions of figure 3 correspond to an electron-rich condition. Thus a difference slightly greater than 1.2 e/kT may be required to satisfy the single-species space-charge criteria. At this time there does not appear to be an unambiguous method of estimating the various work functions and area distribution suited to correlate the electron and ion emission.

The close agreement between the zero-field ion currents at various spacing and temperatures lends credence to the space-charge analytical methods. Agreement of the data heretofore attained only at the close spacing (3 to 11μ) is now attained at a variety of spacings and again supports the observation of a consistent deviation from the Saha-Langmuir relation. Slopes in the space-charge region are obviously unrelated to the Schottky analysis.

Previous observations by Nottingham[12], indicating agreement between isothermal diode theory and ion current measurements at conditions of low ionization probability, are not verified in this study. It should be noted that some of the present results include applied fields that satisfy the Zandberg-Ionov[3] criteria for nonanomalous Schottky effects in the presence of patchy surfaces. These data are the close-spacing data, for which all the spacing calculated from Schottky slopes are within the mechanically measured spacing estimates (figs. 2, 3, and 4).

Houston[13] has suggested that the reduction in ion current with spacing, observed in figure 3, is due to ion-mobility effects rather than space-charge effects. His analysis is in

part based on isothermal diode analysis and the usual continuum-transport relations. In order to judge the applicability of mobility analysis the mean free path must be estimated. From the cross-section equation (eq. (A6)), the mean free path for an ion-neutral encounter (including charge exchange and small angle scattering based on momentum exchange) is about 50μ at T_{cs} of 470° K, 15μ at a T_{cs} of 500° K, and 7μ at a T_{cs} of 530° K. (The relative velocities of atom to ion are assumed to be equivalent to about 0.1 eV in these estimates.) Because of the high accelerating potentials applied (up to 30 V), the velocity gained from the field in one mean free path is greater than the thermal velocities of the particles. It therefore appears that the necessary criterion for conventional mobility analysis does not hold. Indeed the actual mean free path should be larger than the numbers previously cited since the relative velocity may be considerably greater than initially assumed (see kT effect in eq. (A6)). Yet it is obvious that collisional-scattering effects should influence ion transport. The effect is clearly demonstrated in figure 4, where the mean free path is the smallest, and the zero-field space-charge solution for the larger spacings does not agree with the close-spacing values.

No adequate analysis as yet exists for ion transport, which includes electron flow, charge exchange, and velocity-dependent cross section, in the case of few-collisions. Intuitively one can argue that collisional activity can be partially compensated for by electron space charge. To date this appears as the only other explanation of the agreement of single-species space-charge theory with experiment, other than the fact that ions and electrons were not formed at the same surface potentials at the dynamic conditions of the tests.

The analysis of the data of the effective arrival rates in the interelectrode space, presented in figures 5, 6, and 7, is complex. Three particle groups are interacting. The ion group is at temperature T_1 and moves at a velocity dictated by the temperature of the particles and by the difference in surface potentials. The atoms from the collector exist at temperature T_2, while the atoms around the gap are at T_{cs}. The analytical solution of the problem entails all the complexity of a radiation-cavity problem complicated by collisions that are velocity dependent and coupled to applied potentials.

It is expedient, therefore, to look at the extremes. The relative-momentum cross sections of the atom-atom to atom-ion collisions are about 1 to 3 (see eqs. (A5) and (A6)). Thus at low voltages (near zero-surface field), the ion-neutral collision in the gap would appear to dominate because of the high ion density and relatively large cross section. An equilibrium concentration for the cesium particles is probably dictated by momentum exchange between incoming atoms and ions in the interelectrode space. As discussed previously, if flux based on constant pressure between the gap and its surroundings is assumed, approximate agreement between experimental and theoretical ion arrival rates is noted at low fields.

As the voltage is increased, the average residence time of the ion is decreased. It follows that the ion concentration in the gap relative to the atom concentration decreases and the flux balance in and out of the gap shifts toward the atoms. Knudsen flow appears to prevail. Within the framework of the questionable model assumed, the vapor-pressure relations used seem to match the experimental data.

The coupling of arrival rate with applied voltages is not belabored because of any particular practical implications to thermionic-diode performance or as absolute verification of vapor pressure data but only to prevent possible errors of interpretation in some aspects of thermionic-converter diagnostics.

Conclusions

1. Surface ionization of cesium on cesium-coated tungsten surfaces is consistently 3 to 4 times greater than that predicted by the Saha-Langmuir theory.

2. A field-dependent ionization probability is observed following the Schottky mirror-image force relation.

3. The magnitude of the ion current and the applicability of the single-species space-charge theory suggest that ions are formed at a surface of higher work function than are the electrons.

4. At conditions of high-ionization probability the ions couple with the atoms to alter arrival rates on diode surfaces.

Appendix A

Analytical Relations

Richardson Dushman equation

$$J_0 = 120.1 \ T^2 \ \exp(- \ e\varphi/kT) \tag{A1}$$

Schottky equation

$$J = J \ \exp(e\sqrt{eE}/kT) \tag{A2}$$

Boltzmann relation

$$J = J_0 \ \exp(-eV/kT) \tag{A3}$$

Saha-Langmuir equation

$$\alpha = \frac{\nu^+}{\nu_a} = \frac{1}{2} \ \exp\left[(e\varphi - eVi + e \ \sqrt{eE})/kT\right] \tag{A4}$$

Neutral-neutral cross section from Sheldon and Manista[14]

$$\sigma \ = \int_0^\pi 2\pi\sigma(\theta)(1 - \cos \ \theta)(\sin \ \theta)d\theta \tag{A5a}$$

Neutral-neutral cross section with $\sigma(\theta)$ values of reference 14

$$\sigma_m = 470 \ \overset{\circ}{A}{}^2 \quad \text{at} \quad 400^\circ \ K \tag{A5b}$$

Ion-neutral cross section from Sheldon[15]

$$\sigma_{+,n} = 2A^2 - 4AB \left(\frac{3}{2} - \epsilon + \ln k'T\right) + B^2\left[4\left(\frac{3}{2} - \epsilon\right)\ln k'T \right.$$
$$\left. + 2(\ln k'T)^2 + \kappa\right] + \left(\frac{\pi}{2}\right)^2 \frac{e^2\alpha}{B^2k'T\left(\frac{A}{B} - \ln k\bar{T}\right)^2} \tag{A6}$$

$$\sigma_{+,n} \approx 1400 \ \overset{\circ}{A}{}^2 \quad \text{at} \quad k'T = 0.1 \ eV$$

Cesium vapor pressure relations from Heimel[8]

$$\log_{10} p \ (\text{newtons/sq m}) = - \ \frac{4053.3}{T} - 0.915282 \ \log_{10}T + 12.05025 \tag{A7}$$

The Langmuir space-charge relation[16] $\chi = \mathscr{F}(\psi)$ expanded in terms of usual variables for a singly charged cesium ion

$$(1.442 \times 10)J^{1/2} \times T^{-3/4} = \mathscr{F}\left(\frac{eV}{kT}\right) \tag{A8}$$

The symbol χ as a function of ψ is tabulated in several references (e.g., Nottingham[17]).

Free energy per particle (Boltzmann statistics)[1]

$$\mu = kT \ \ln\left(\frac{h^2}{2\pi mkT}\right)^{3/2} \frac{n}{Q} \tag{A9}$$

References

1. Mayer, J. E., and Mayer, M. G.: "Statistical Mechanics." John Wiley & Sons, Inc. (New York) 1940

2. Copley, M. J., and Phipps, T. E.: Phys. Rev. 48, 960 (1935)

3. Zandberg, E. Ia., and Ionov, N. I.: Soviet Physics Uspehki 67, 255 (1959)

4. Nottingham, W. B.: Sheath and Plasma Theory of an Isothermal Diode. Rep. 4-62, Thermo Electron Eng. Corp. Oct. (1962)

5. Kaminsky, M.: "Atomic and Ionic Impact Phenomena on Metal Surfaces." Academic Press Inc. (New York) 1965

6. Zandberg, E. Ia., and Ionov, N. I.: The Surface Ionization of Lithium Atoms on Polycrystalline Tungsten in Electric Fields up to 1.3 X 10^6 v/cm. Soviet Phys.-Techn. Physics $\underline{3}$, 2243 (1958)

7. Breitwieser, R., Rept. 23rd Annual Conf. on Phys. Electronic, M.I.T. (1963)

8. Heimel, Sheldon: Thermodynamic Properties of Cesium up to 1500° K.   NASA TN D-2906, 1965

9. Nottingham, Wayne B., and Breitwieser, Roland: "Theoretical Background for Thermionic Conversion Including Space-Charge Theory, Schottky Theory, and the Isothermal Diode Sheath Theory." Proposed NASA Technical Note.

10. Goldstein, C.: Private Communication

11. Goldstein, C. M.: "Theoretical Current-Voltage Curve in Low-Pressure Cesium Diode for Ion-Rich Emission." Report on the Thermionic Conversion Specialist Conference, Gatlinburg (Tenn.) (Oct. 1963)

12. Nottingham, W. B.: "Cesium Ion Production in a Strong Ion Accelerating Field." 23rd Annual Conf. on Phys. Electronics, M.I.T. (1963)

13. Houston, J. M., and Webster, H. F.: Thermionic Converter Research Studies. Final Report, General Electric Co., Air Force, Cambridge Research Lab. Bedford, Mass., AFCRL 64-409, Oct. 1964

14. Sheldon, John W., and Manista, Eugene J.: Atomic Beam Determination of the Cesium-Cesium Total Scattering Cross Section. Proposed NASA Technical Note.

15. Sheldon, John W.: Mobility of Positive Ions in Their Own Gas: Determination of Average Momentum-Transfer Cross Section. NASA TN D-2408, 1964

16. Langmuir, I.: Phys. Rev. $\underline{21}$, 419 (1923)

17. Nottingham, W. B.: Thermionic Emission. Rep. 321, Res. Lab. of Electronics, M.I.T. (1956)

E-3232

E-3232

EXP. SAT. ION CURRENT DENSITY, A/SQ CM

10^{-1}
10^{-2}
10^{-3}
10^{-4}
10^{-5}
10^{-6}

Cs RESERVOIR
TEMP,
°K

○ 470
◇ 500
□ 530

SAHA LANGMUIR

CS-37550

10^{-6} 10^{-5} 10^{-4} 10^{-3} 10^{-2} 10^{-1}
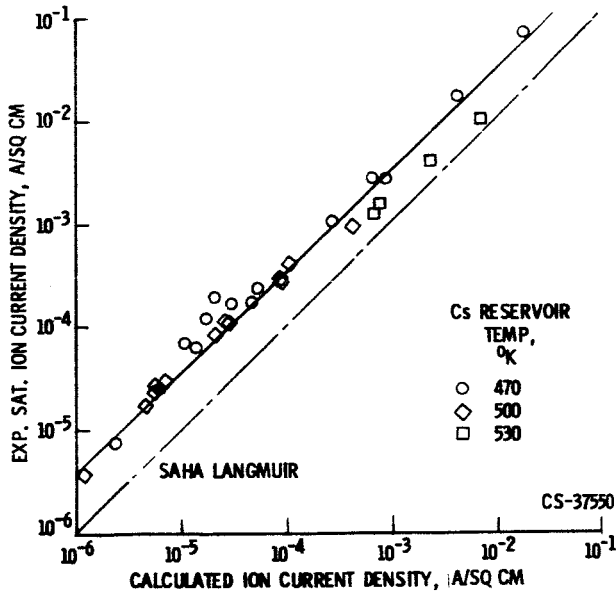CALCULATED ION CURRENT DENSITY, A/SQ CM

FIGURE 1. - COMPARISON OF ANALYTICAL AND EXPERIMENTAL
ZERO-FIELD ION CURRENTS IN A CESIUM-TUNGSTEN DIODE;
EMITTER TEMPERATURES, 1350 TO 1650° K; INTERELECTRODE
SPACING, 3 TO 11 μ.

ZERO-FIELD POTENTIALS

LOG ION CURRENT DENSITY, 4 + LOG$_{10}$ J, A/SQ CM

SPACING, μ
1.6
1.5
1.4 — INFLUENCE
OF
1.3 — ELECTRON
CURRENT
1.2
1.1
1.0
.9

10
3-11
227
113
227

DATA
10 μ
SCHOTTKY
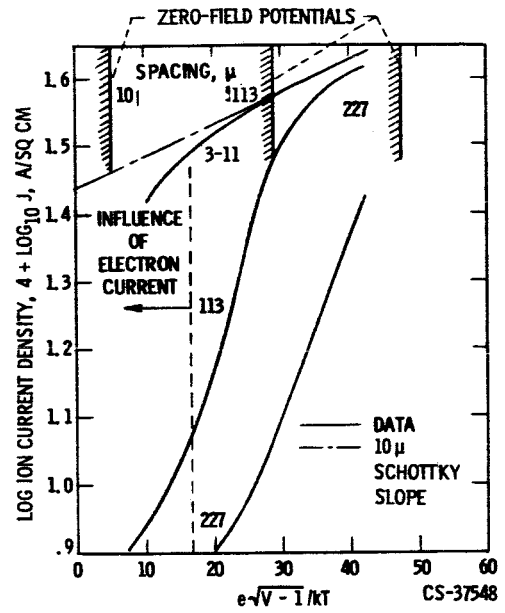SLOPE

0 10 20 30 40 50 60
e√V - 1 /kT   CS-37548

FIGURE 2. - SCHOTTKY PLOTS OF ION CURRENT
SHOWING ZERO-FIELD INTERCEPTS BASED ON
SINGLE-SPECIES SPACE-CHARGE ANALYSIS;
EMITTER TEMPERATURE, 1530° K; CESIUM RESER-
VOIR TEMPERATURE, 470° K.

ZERO-FIELD POTENTIALS   SPACING, μ

ION CURRENT DENSITY 4 + LOG$_{10}$ J, A/SQ CM

.8
.7
.6
.5
.4
.3
.2
.1
0
-.1
-.2

10
57
113
226

3-11
57
113
226

INFLUENCE
OF
ELECTRON
CURRENT

LANGMUIR-
SAHA
THEORY

ZERO FIELD
INTERCEPT
AT 41.6

INTERCEPT
AT 61.0

450

790

DATA
10 μ SCHOTTKY
SLOPE

0 4 8 12 16 20 24 28 32 36
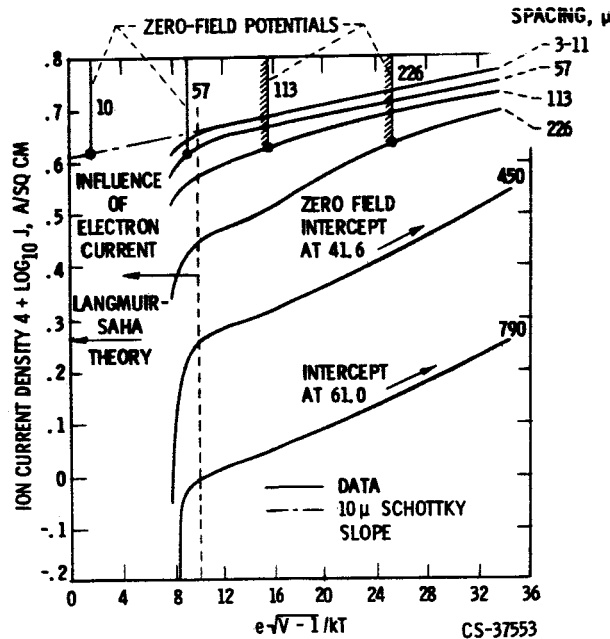e√V - 1 /kT   CS-37553

FIGURE 3. - SCHOTTKY PLOTS OF ION CURRENT SHOWING
ZERO-FIELD INTERCEPTS BASED ON SINGLE-SPECIES
SPACE-CHARGE ANALYSIS AT NOMINALLY ELECTRON-
RICH EMISSION CONDITION; EMITTER TEMPERATURE,
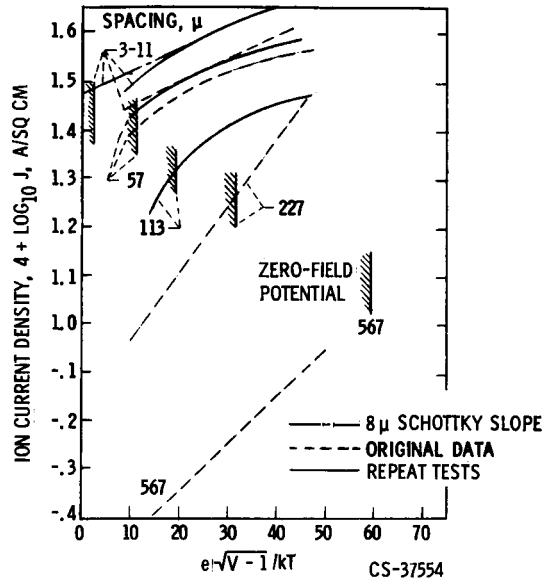1500° K, CESIUM-RESERVOIR TEMPERATURE, 500° K.

FIGURE 4. - SCHOTTKY PLOTS OF ION CURRENT
SHOWING ZERO-FIELD INTERCEPTS BASED ON
SINGLE-SPECIES SPACE-CHARGE ANALYSIS;
CESIUM PRESSURE CORRESPONDING TO
CONDITIONS OF SIGNIFICANT ATOM-ION
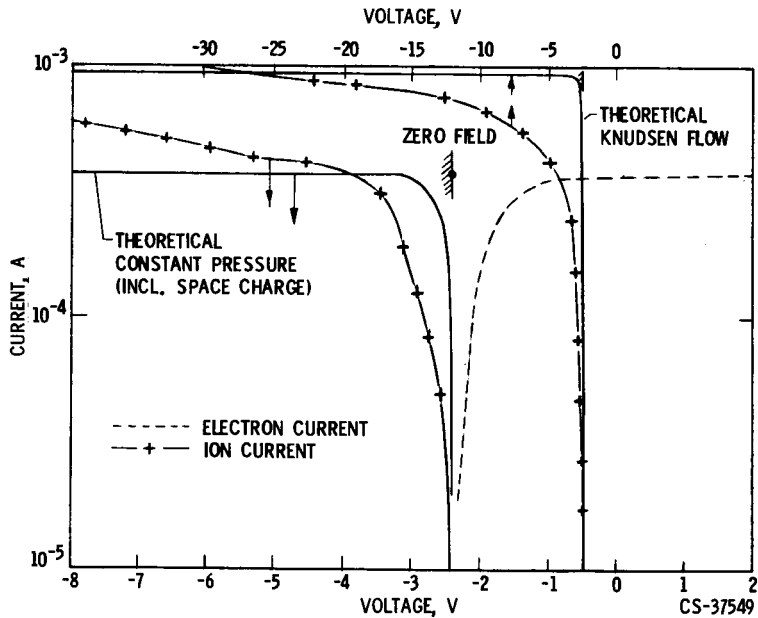COLLISIONS; EMITTER TEMPERATURES, 1600°
K; CESIUM TEMPERATURE, 530° K.

Figure 4 axis labels and legend:

ION CURRENT DENSITY, $4 + LOG_{10}$ J, A/SQ CM

SPACING, μ

3-11

57

113

227

ZERO-FIELD POTENTIAL

567

567

— 8μ SCHOTTKY SLOPE
--- ORIGINAL DATA
—— REPEAT TESTS

$e\sqrt{V-1}/kT$

Figure 5 axis labels and legend:

VOLTAGE, V

CURRENT, A

THEORETICAL KNUDSEN FLOW

ZERO FIELD

THEORETICAL CONSTANT PRESSURE (INCL. SPACE CHARGE)

----- ELECTRON CURRENT
—+— ION CURRENT

VOLTAGE, V

FIGURE 5. - EFFECT OF APPLIED VOLTAGE ON PARTICLE ARRIVAL RATES; EMITTER
TEMPERATURE, 2007° K; EMITTER WORK FUNCTION, 4.92 V; SPACING, 3 TO 11 μ;
CESIUM-RESERVOIR TEMPERATURE, 329° K; EMITTER AREA, 1.765 SQ. CM.

E-3232

VOLTAGE, V

-40 -35 -30 -25 -20 -15 -10 -5 0 5 10

10^{-3}

KNUDSEN FLOW

ZERO
FIELD

CONSTANT PRESSURE

CURRENT, A

10^{-4}

——— EXPERIMENT
- - - THEORY

10^{-5}

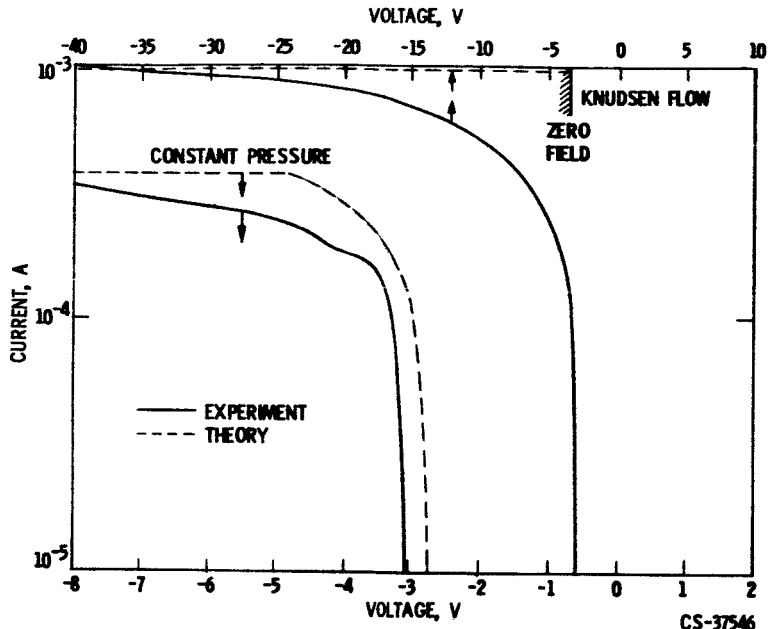-8 -7 -6 -5 -4 -3 -2 -1 0 1 2

VOLTAGE, V

CS-37546

FIGURE 6. – EFFECT OF APPLIED VOLTAGE ON PARTICLE ARRIVAL RATES; EMITTER
TEMPERATURE, 2003° K; EMITTER WORK FUNCTION, 4.92; SPACING, 113 μ;
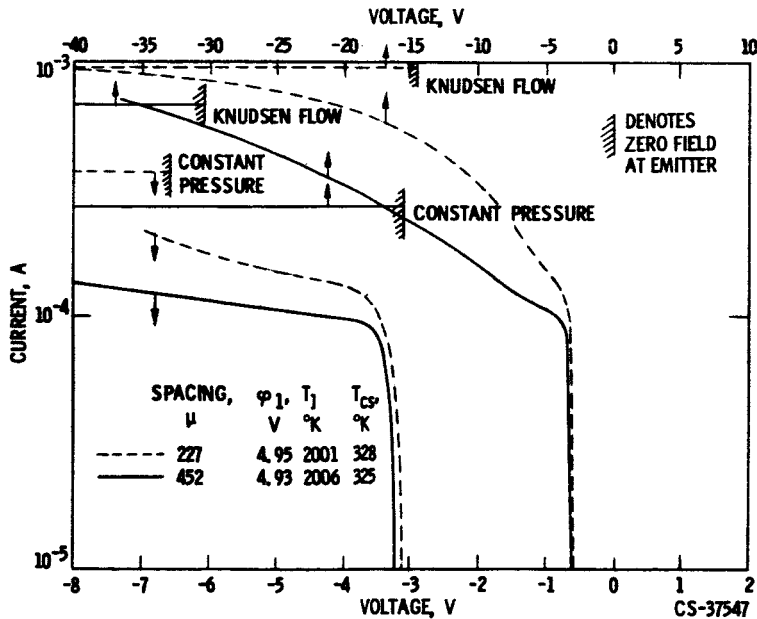CESIUM RESERVOIR TEMPERATURE, 329° K; EMITTER AREA, 1.765 SQ. CM.

VOLTAGE, V

-40 -35 -30 -25 -20 -15 -10 -5 0 5 10

10^{-3}

KNUDSEN FLOW

KNUDSEN FLOW

DENOTES
ZERO FIELD
AT EMITTER

CONSTANT
PRESSURE

CONSTANT PRESSURE

CURRENT, A

10^{-4}

SPACING, μ	φ_1, V	T_1, °K	T_{cs}, °K
- - - 227	4.95	2001	328
——— 452	4.93	2006	325

10^{-5}

-8 -7 -6 -5 -4 -3 -2 -1 0 1 2

VOLTAGE, V

CS-37547

FIGURE 7. – EFFECT OF APPLIED VOLTAGE ON PARTICLE ARRIVAL RATES; INTER-
ELECTRODE SPACING, 227 AND 452 μ; EMITTER AREA, 1.765 SQ. CM.